Available online at www.sciencedirect.com
SCIENCE DIRECT®
Electrochemistry Communications 5 (2003) 940–945
electrochemistry communications
www.elsevier.com/locate/elecom

Improving the high-temperature performance of $LiMn_2O_4$ spinel electrodes by coating the active mass with MgO via a sonochemical method

J.S. Gnanaraj, V.G. Pol, A. Gedanken, D. Aurbach *

Department of Chemistry, Bar-Ilan University, Ramat-Gan 52900, Israel

Received 6 August 2003; accepted 19 August 2003
Published online: 30 September 2003

Abstract

$LiMn_2O_4$ spinel coated sonochemically with MgO was studied as an active mass in composite cathodes in standard Li electrolyte solutions for Li-ion batteries at 60 °C. Solutions comprising 1 M $LiPF_6$ in a mixture of ethylene, dimethyl, and diethyl carbonates (EC–DMC–DEC; 2:2:1) were used. It was possible to obtain $LiMn_2O_4$ particles fully covered by porous magnesia films that allow a free transport of Li-ions. Electrodes comprising $LiMn_2O_4$, modified by MgO showed a higher capacity retention compared to the electrodes comprising an uncoated active mass, specially at elevated temperatures. We suggest that the presence of an MgO film on the surface of the $LiMn_2O_4$ particles, reduces the detrimental effect of HF contamination present in $LiPF_6$ solutions, reduces the electrodes' impedance and improves their kinetics.

Keywords: Spinel $LiMn_2O_4$ electrodes; Sonochemical coating; MgO; $LiPF_6$; EC; DEC; DMC; Impedance spectroscopy; Surface films; Li-ion batteries

1. Introduction

$LiMn_2O_4$ spinel has been realized as a promising cathode material for lithium-ion batteries because of promising properties such as low cost, abundant precursors, non-toxicity and environmental benignness [1,2]. However, $LiMn_2O_4$ electrodes in the 4 V (vs. Li/Li^+) region suffer from capacity fading, especially at elevated temperatures, mainly due to detrimental surface reactions with acidic contaminants in the electrolyte solutions, and dissolution of manganese that leads to detrimental structural changes of the active mass [3,4]. $LiPF_6$ itself always brings with it HF contamination, which is detrimental to the performance of both negative and positive electrodes [5]. We discovered that $LiMO_2$ cathode materials (M = Co, Ni, Mn, etc.) may react spontaneously with solution species, resulting in the formation of surface films [6]. Hence, it appears that Li-ion battery cathodes are also SEI-type electrodes [7] namely, their electrochemical behavior may be controlled by surface films through which Li-ion transport takes place. Major possible surface reactions of the cathodes may be driven by chemical properties of both their active mass and solution species. For instance, HF reacts with $LiMO_2$ cathode materials to form surface LiF, and some of the cathode materials, e.g., $LiNiO_2$, are nucleophilic and attack the electrolytic alkyl carbonate molecules, thus forming $-OCO_2Li$ surface groups and/or inducing formation of polymeric species such as polycarbonates [6,7]. It should be noted that the capacity fading found for both Li–C and $LiMO_2$ electrodes in Li-ion batteries is largely due to surface phenomena related to the above reactions. Too intensive surface films formation may increase the electrodes' impedance and even isolate electrically part of the active mass [8]. At elevated temperatures, the above-described

* Corresponding author. Fax: +972-3-5351250.
E-mail address: aurbach@mail.biu.ac.il (D. Aurbach).

1388-2481/$ - see front matter © 2003 Elsevier B.V. All rights reserved.
doi:10.1016/j.elecom.2003.08.012

surface phenomena occur even more intensively; higher electrode impedance may be developed, and pronounced surface-related capacity fading of electrodes in Li-ion batteries can be observed. Several methods for improving the stability and cycleability of $LiMn_2O_4$ spinel cathodes have been investigated. Among them, partial substitution of Mn ions (doping) by other metal ions and surface modification of the active material may improve the cycling performance [9–11]. Coating of the surface of $LiMn_2O_4$ particles by surface species such as $LiCoO_2$ [12], V_2O_5 [13], Al_2O_3 [14], SiO_2 [15], and MgO [16], in order to improve the cycling performance of $LiMn_2O_4$ electrodes was reported. Most of these coating were performed through chemical processes, solution-based techniques such as sol–gel transformation, solution precipitation, and micro-emulsion [9–16]. Sonochemical methods are relatively new, simple, and operate at ambient conditions [17]. They are widely used for the synthesis of nanoparticles [18–20]. Sonochemical methods can also be used for the uniform coating of materials' surfaces [21–23]. This method is based on the phenomenon of acoustic cavitation, which involves the formation, growth, and collapse of bubbles in liquid, in which extreme conditions, such as very high transients temperatures, which may exceed 5000 °C [24] in localized hot spots, and an ultrafast cooling rate, >1000 °C/s can be obtained. Ultrasound radiation also induces very efficient agitation of reaction mixtures [25]. We report herein on a sonochemical method of surface modification of $LiMn_2O_4$ particles by coating them with a thin layer of MgO. This coating seems to improve their performance as a cathode material for Li-ion batteries at elevated temperatures.

2. Experimental

The $LiMn_2O_4$ spinel powder (particle size of 5–10 mM) was obtained from Merck KGaA (highly pure, Li battery grade) and was used as received. Ammonium hydroxide (99.99%) and $(CH_3CO_2)_2Mg \cdot 4H_2O$ (99.99%) were obtained from Aldrich Chemical Co. and were used as received. For the preparation of coated materials, 500 mg of $LiMn_2O_4$ were first sonicated for 10 min in order to disperse all particles in 100 ml of doubly distilled water. The required amount of precursors $MgSO_4 \cdot 4H_2O$ or $(CH_3CO_2)_2Mg \cdot 4H_2O$ (0.5–10% molar vs. $LiMn_2O_4$), was added to the above solution, followed by further sonication (120 min). A VCX 600 sonicator from Sonic and Materials, 20 kHz, 40 W/cm^2 was used. A total of 7–10 ml of 24% (by weight) aqueous ammonia was added dropwise during the sonication. The product was centrifuged, washed thoroughly twice with doubly distilled water, and dried in vacuum. The as-prepared samples were further dried at 450 °C under air for 4 h before use.

XRD measurements were performed with the D8 Advanced Powder X-ray Diffractometer from Bruker Inc. (Cu $K\alpha = 1.5418$ Å radiation). The morphology of the particles and the surface coating were studied by transmission electron microscopy (TEM, JEOL-JEM 100 SX microscope working at 100 kV). Thermogravimetric analysis was carried out under nitrogen with a TGA/STDA 851 system from Mettler Inc. Differential scanning calorimetry (DSC) was performed using a Mettler DSC 25 system (TC15 TA controller) instrument in the temperature range of 30–600 °C at a scan rate of 5 °C/min. The magnesium content of the products was examined with a Perkin–Elmer atomic absorption spectrometer (AAS) with a magnesium lamp (Beckman make) operating at $\lambda = 202.6$ nm. The solutions for the AA were prepared by dissolving 100 mg of magnesium-coated $LiMn_2O_4$ powder in 10 ml of conc. HCl and 10 ml of H_2O_2, followed by diluting to 1300 ml in pure water.

For surface analysis studies, we used a Magna 860 (Nicolet) FTIR spectrometer placed in a glove box under H_2O and CO_2-free atmosphere (fed by compressed air, treated with a Balston Inc., Model A-05881 air purifier). The powder samples were analyzed by diffuse reflectance mode (a DRIFT accessory from Harrick Inc.). The cathodes were comprised of $LiMn_2O_4$ (70 wt%), 15 wt% graphite powder (KS-6 Timrex Inc.), 5 wt% carbon black (conductive additives), 10 wt% PVdF binder, and an aluminum foil (Goodfellow, England) current collector. Slurries containing the active mass and the binder were prepared using *N*-methyl pyrrolidone (Fluka Inc.) and were coated on the appropriate current collectors, as already described [6–8]. The electrodes were dried in an oven at 140 °C and were then transferred to the glove box (VAC Inc., highly pure argon atmosphere H_2O and O_2 at the ppm level). The 1 M $LiPF_6$ solution in a mixture of EC–DEC–DMC (2:1:2 by volume) was obtained from Merck KGaA (highly pure, Li battery grade) and could be used as received. The electroanalytical characterizations of the electrodes were performed either in three-electrode cells based on standard coin-type cells (Model 2032, NRC Canada, ϕ 19 mm), or parallel plate cells made of polyethylene. In the coin cells, a Li wire reference electrode was pasted onto a nickel wire, which was placed between the working electrode and the Li foil counter electrode, covered by a separator (Celgard 2400). These cells were hermetically sealed using the 2324 Coin Cell crimper from NRC/ICPET. In the polyethylene cells, the working electrode was surrounded symmetrically on both sides by a Li foil counter electrode, and a Li wire served as a reference electrode.

Freshly prepared, thin $LiMn_2O_4$ electrodes with OCV around 3.3 V (vs. Li/Li^+) were initially aged by voltammetric cycling between 3.5 and 4.25 V (vs. Li/Li^+) for five times at 1 mV/s before the rigorous

electrochemical measurements. Prolonged galvanostatic cycling was performed at C/10 or C/2 rates in coin-type cells at 30 and 60 °C in incubators (Carbolite Inc., Model PIF30-200) using A Maccor multichannel system (Model 2000). For voltammetric and impedance measurements, Autolab Model PGSTAT20 Electrochemical systems equipped with frequency response analyzers (FRA), driven by Pentium II IBM PC were used. The amplitude of the ac voltage was 3 mV and the electrodes were measured at a constant base potential after the appropriate equilibration.

3. Results and discussion

Using 2, 5, 10, and 15 mol% of magnesium acetate vs. $LiMn_2O_4$ in the solution mixtures provided an active solid mass containing MgO at 1.3, 4.2, 5.5, and 5.6 mol% (respectively) of the $LiMn_2O_4$, as was analyzed by atomic absorption. FTIR studies showed that the sonochemical products are $LiMn_2O_4$ containing $Mg(OH)_2$ (a typical υ_{OH} peak at 3647–3697 cm^{-1}). Upon heating, the $Mg(OH)_2$ is converted to MgO (FTIR spectra of the samples heated to 450 °C do not have this υ_{OH} peak). Fig. 1 shows typical TGA and DSC curves of the sonochemically coated $LiMn_2O_4$ in a solution containing 5.5% MgO. The TGA and DSC measurements were carried out at a heating rate of 10 °C/min and at 5 °C/min, respectively. The as-prepared sample (i.e., the sonochemical product) showed a three-step weight loss in the temperature range of 40–1000 °C. The first weight loss around 0.5% in the temperature range of 50–120 °C is associated with the removal of absorbed water (see the corresponding endotherm in the DSC curve). The second weight loss, of 1% in the 280–350 °C range, and the corresponding endotherm in the DSC curve are associated with the transformation of the $Mg(OH)_2$ coating to MgO by condensation. (The $Mg(OH)_2$ is formed by the reaction of magnesium acetate or sulfate precursor in the aqueous medium.) The third weight loss, of 5.3% in the range of 820–940 °C should be related to a partial decomposition of the $LiMn_2O_4$ to Li–Mn–O compounds containing a higher concentration of Mn^{3+}, based on reports on the thermal decomposition of $LiMn_2O_4$, which involves evolution of oxygen at high temperatures [26].

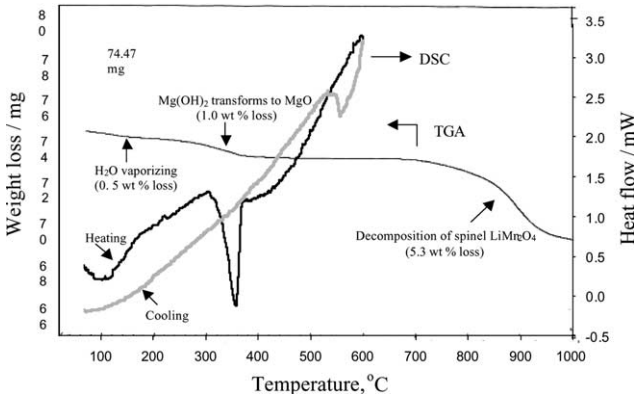

Fig. 1. TGA and DSC curves for the MgO-coated $LiMn_2O_4$ materials measured between the temperature range of 40 and 1000 °C at the scan rates of 10 and 5 °C/min, respectively.

The XRD diffraction patterns of the sonochemical products ($LiMn_2O_4$ containing $Mg(OH)_2$) and the products heated to 450 °C ($LiMn_2O_4$ containing MgO) were very similar to the patterns of the pristine $LiMn_2O_4$. We could not detect patterns of $Mg(OH)_2$ or MgO, probably due to the fact that the highest content of these Mg compounds in the samples did not exceed 5.6 mol%. XRD patterns of samples heated to 1000 °C reflect the partial decomposition of $LiMn_2O_4$ (e.g., the patterns include Mn_3O_4 peaks).

Fig. 2 compares TEM micrographs of pristine $LiMn_2O_4$ and MgO-coated (5.5%) $LiMn_2O_4$ particles (a and b, respectively). Fig. 2c shows the MgO layer at a higher magnification. From these studies it seems that the modified $LiMn_2O_4$ particles are completely covered with a thin, porous layer of MgO. From the XRD and the TEM studies, we assume that the active mass obtained by the sonochemical reaction and the consequent heating up to 450 °C, produces $LiMn_2O_4$, whose structure remains unchanged, coated by a porous, non-uniform magnesia surface film. When the reaction mixture contained a magnesium source at an amount around 10% (molar) vs. $LiMn_2O_4$, a completed coverage of the $LiMn_2O_4$ by magnesia was obtained.

Electrochemical measurements of composite electrodes comprising pristine and MgO-coated $LiMn_2O_4$ were performed at 30 and 60 °C. The tests included fast and slow scan rate CV, chronopotentiometry (i.e., galvanostatic charge–discharge cycling), and impedance spectroscopy. In general, these electrodes could deliver an initial capacity higher than 120 mAh/g. At 30 °C we could not see a pronounced difference between coated and uncoated electrodes. The initial capacity of the electrodes comprising MgO-coated $LiMn_2O_4$ was generally slightly lower, but more stable upon repeated cycling, compared to that of reference electrodes (uncoated active mass). Pronounced differences in the behavior of the electrodes were seen at elevated temperatures. Hence, below we concentrate on the presentation of some results obtained at 60 °C.

At elevated temperatures (e.g., >50 °C) the capacity fading of regular $LiMn_2O_4$ electrodes in standard solutions (containing $LiPF_6$) upon repeated cycling, is pronounced [3,4]. Fig. 3 shows typical cycle life curves of these electrodes obtained in galvanostatic cycling at 60 °C. Electrodes comprising uncoated $LiMn_2O_4$ and coated $LiMn_2O_4$ containing different amounts of MgO (indicated) are compared in the figure. It is clear from

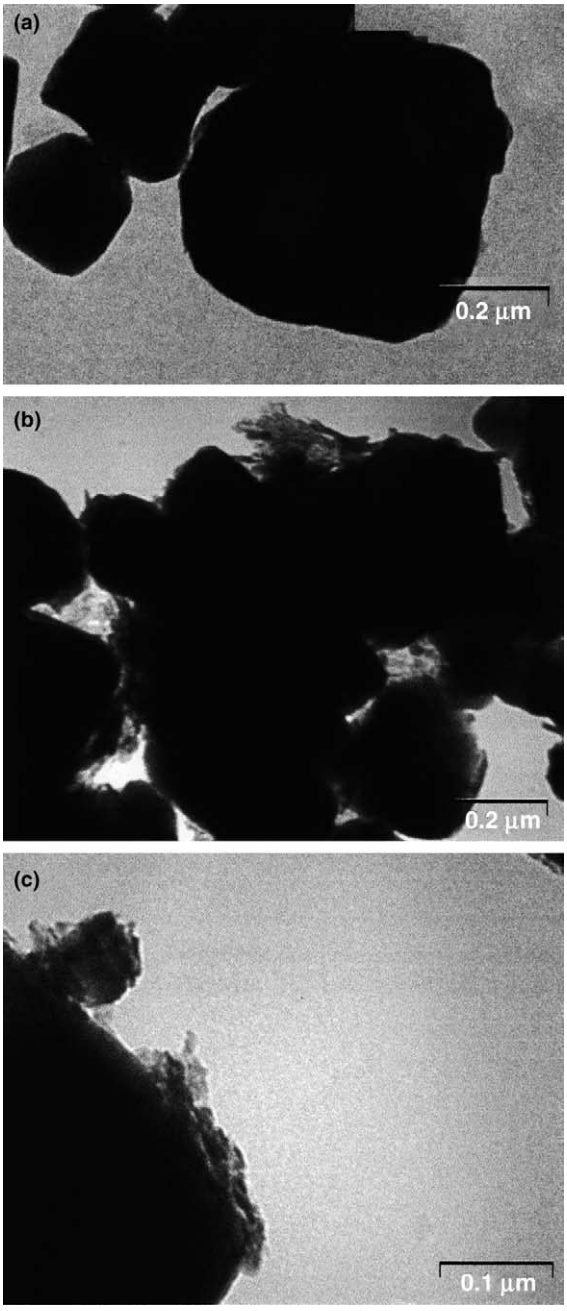

Fig. 2. TEM micrographs of pristine uncoated $LiMn_2O_4$ powder, and MgO (5.5%)-coated $LiMn_2O_4$ particles (a and b, respectively). Micrograph 4(c) shows the MgO layer at higher magnification.

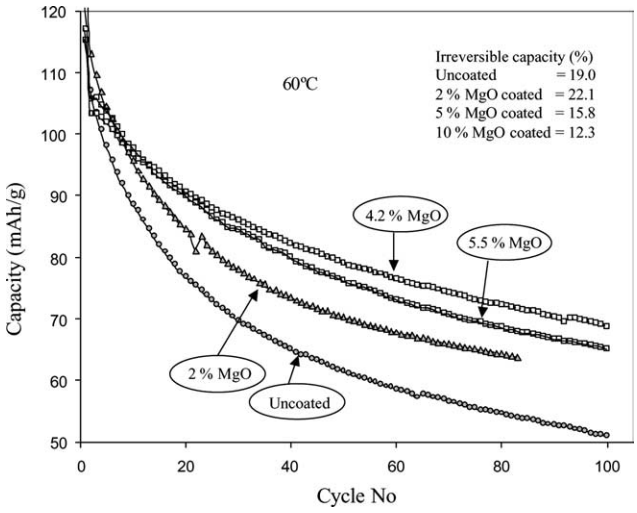

Fig. 3. Typical cycle life curves (galvanostatic cycling, capacity vs. cycle number) of $LiMn_2O_4$ electrodes comprising coated and uncoated active mass (indicated). Coin-type cells, 60 °C, Li metal counter electrodes, EC–DEC–DMC (2:1:2) 1 M $LiPF_6$ solutions, C/2 rates.

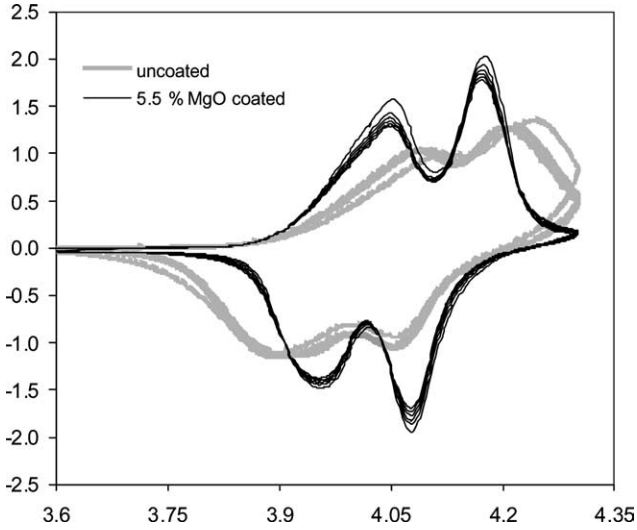

Fig. 4. First five consecutive cyclic voltammograms of electrodes comprising uncoated (shadow line) and 5.5% MgO-coated (solid line) $LiMn_2O_4$ at 60 °C (lithium as counter and reference electrodes) between 3.7 and 4.30 V at a scan rate of 1 mV/s in EC–DEC–DMC (2:1:2) 1 M $LiPF_6$ solutions.

this figure that the capacity fading of electrodes containing MgO-coated $LiMn_2O_4$ is much less pronounced than that of electrodes comprising regular, uncoated $LiMn_2O_4$ particles.

Fig. 4 shows five consecutive CVs of electrodes comprising MgO-coated (5.5%) and uncoated $LiMn_2O_4$ (1 mV/s), measured at 60 °C. These CVs show two sets of peaks, which reflect the typical redox processes of these electrodes in the 4 V (vs. Li/Li^+) domain, which involves phase transitions [1,2,7]. As is seen in this figure, the CV peaks related to the MgO-coated active mass are much sharper and appear with much smaller hysteresis, compared to the peaks of the electrode comprising uncoated $LiMn_2O_4$. These differences mean that the kinetics of the MgO-coated active mass is faster than that of the standard, uncoated material.

Fig. 5 shows families of Nyquist plots measured with MgO-coated (% MgO is indicated) and uncoated $LiMn_2O_4$ electrodes at 60 °C at different equilibrium

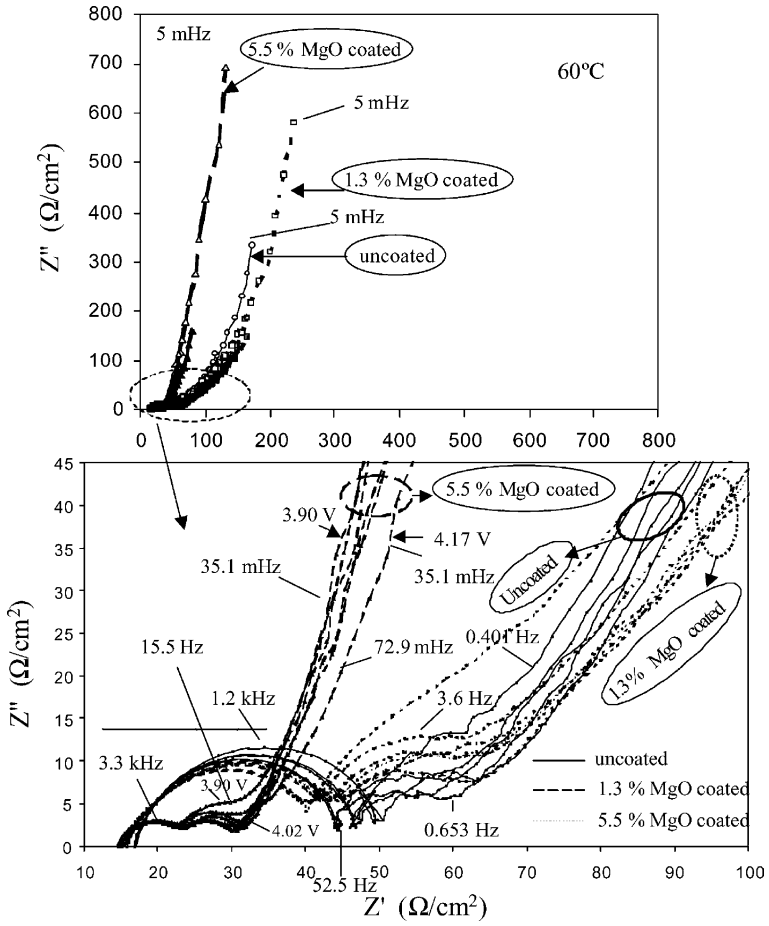

Fig. 5. A family of Nyquist plots obtained from $LiMn_2O_4$ electrodes at different equilibrium potentials in EC–DEC–DMC (2:1:2) 1 M $LiPF_6$ solutions at 60 °C. These series of experiments were carried out after the electrodes were cycled (CV) in the potential range of interest, during which its surface chemistry was stabilized. Some frequencies are also marked near the spectra. The relevant potentials and MgO contents are indicated.

potentials (indicated). These Nyquist plots are very typical of these electrodes. They reflect the serial nature of Li insertion–deinsertion processes into $LiMn_2O_4$ electrodes, as already demonstrated and discussed in detail [6,7]. At the high-medium frequencies, two flat semicircles, reflect Li migration through surface layers (the high-frequency semicircle) and interfacial charge transfer (the medium semicircle). At the low frequencies, a 'Warburg'-type element (linear Z'' vs. Z' behavior) in the spectra reflects the solid-state diffusion of Li-ions into the bulk $LiMn_2O_4$ particles. Finally, at the very low frequencies, the Nyquist plots behave as very steep Z'' vs. Z' straight lines that reflect the electrodes' capacitive behavior, namely, accumulation of charge due to Li delithiated or lithiation. When the content of the MgO is too low, the difference between the impedance of electrodes comprising coated or uncoated $LiMn_2O_4$ particles is negligible. At a sufficiently high concentration of MgO in the active mass (e.g., 5.5%, see Fig. 5), the impedance of the electrodes comprising MgO-coated $LiMn_2O_4$ was much lower than that of the reference electrodes. These results correlate well with the CV measurements that demonstrated faster kinetics for the MgO-coated active mass. As already discussed in detail [27], these electrodes are covered by surface films formed by spontaneous reactions between their active mass and solution species. Highly important in this respect are acid–base reactions between lithiated oxide and trace HF in solution, which form highly resistive LiF surface films. We assume that the basic MgO coating protects the active mass from such reactions and neutralized acidic contaminants. The sonochemical process leads to the formation of a sufficiently porous MgO film that protects the particles' surface from detrimental reactions, but not on the account of fast transport of Li-ions.

4. Conclusion

In this communication, we present preliminary results that demonstrate a relatively easy and efficient proce-

dure to produce $LiMn_2O_4$ particles coated by nanosized magnesia. Sonication of slurries comprising $LiMn_2O_4$ particles and magnesium sources such as $MgSO_4$ or Mg acetate, produces $LiMn_2O_4$ coated by a $Mg(OH)_2$ film. Further heating of this product to 450 °C transforms the $Mg(OH)_2$ to MgO, thus producing magnesia-coated $LiMn_2O_4$. When the amount of the Mg source in the slurries is around 10% (molar) of the $LiMn_2O_4$, the $LiMn_2O_4$ particles become fully covered by a porous MgO film (about 5.5% molar of the $LiMn_2O_4$ mass). Structural studies of these materials by XRD and TEM show that the above processes do not change the $LiMn_2O_4$ structure. The products are indeed $LiMn_2O_4$ particles coated by surface films of MgO with distinctive boundaries. The MgO-coated $LiMn_2O_4$ behaves better than regular $LiMn_2O_4$ as a cathode material in standard Li-ion battery solutions ($LiPF_6$ in alkyl carbonate mixtures) at elevated temperatures. The impedance of electrodes comprising MgO-coated $LiMn_2O_4$ is lower and their kinetics is faster than regular $LiMn_2O_4$ electrodes. The capacity fading of MgO-coated $LiMn_2O_4$ electrodes at elevated temperatures is much smaller compared to regular $LiMn_2O_4$ electrodes. We assume that the basic MgO film protects the $LiMn_2O_4$ from detrimental reactions with acidic solution species, which usually form resistive surface films that increase the electrodes' impedance. Fortunately, the MgO films thus formed are sufficiently porous to allow free transport of Li-ions to the active mass.

It should be emphasized that the results presented herein are preliminary. Further optimization and testing are needed in order to extract the potential of the above procedure for the production of a highly attractive cathode material of Li-ion batteries.

Acknowledgements

Partial support for this work was obtained from the BMBF, the German Ministry of Science, in the framework of the DIP program for Collaboration Between Israeli and German Scientists, and by the EC in the framework of the fifth program (the NanoBatt project).

References

[1] J.M. Tarascon, D. Guyomard, Electrochem. Acta 38 (1993) 1221.
[2] M.M. Thackeray, Prog. Solid State Chem. 25 (1997) 1.
[3] P. Arora, R.E. White, M. Doyle, J. Electrochem. Soc. 145 (1998) 3647.
[4] V. Manev, B. Banov, A. Momchiler, A. Nassalevska, J. Power Sources 57 (1995) 99.
[5] K. Kanamura, H. Tamura, Z. Takehara, J. Electroanal. Chem. 333 (1992) 127;
A. Du Pasuier, A. Blyr, P. Courjal, D. Larccher, G. Amatucci, B. Gerand, J.M. Tarascon, J. Electrochem. Soc. 146 (1999) 428.
[6] D. Aurbach, K. Gamolsky, B. Markovsky, G. Salitra, Y. Gofer, J. Electrochem. Soc. 147 (2000) 1322.
[7] D. Aurbach, M.D. Levi, E. Levi, H. Teller, B. Markovsky, G. Salitra, L. Heider, U. Heider, J. Electrochem. Soc. 145 (1998) 3024.
[8] D. Aurbach, B. Markovsky, A. Rodkin, M. Cojocaru, E. Levi, H.J. Kim, Electrochim. Acta 47 (2002) 1899.
[9] M. Wakihara, G. Li, H. Ikuta, in: M. Wakihara, O. Yamamoto (Eds.), Lithium Batteries – Fundamentals and Performance, Kodansha/Wiley-VCH, Japan/Germany, 1998, p. 26.
[10] C. Sigala, A.L.G.L. Salle, Y. Piffard, D. Guyomard, J. Electrochem. Soc. 148 (2001) A826.
[11] G.G. Amatucci, N. Pereira, T. Zheng, J.M. Tarascon, J. Electrochem. Soc. 148 (2001) A171.
[12] Z. Liu, H. Wang, L. Fang, J.Y. Lee, L.M. Gan, J. Power Sources 104 (2002) 101.
[13] H. Kweon, G. Kim, D. Paark, U. Pat. 6,183,911 (2001).
[14] J. Cho, Y.J. Kim, T.J. Kim, B. Park, Chem. Mater. 13 (2001) 18.
[15] Z. Zheng, Z. Tang, Z. Zhang, W. Shen, Y. Lin, Solid State Ionics 148 (2002) 317.
[16] A.M. Kannan, A. Manthiram, Electrochem. Solid-State Lett. 5 (2002) A167.
[17] S. Avivi, Y. Mastai, G. Hodes, A. Gedanken, J. Am. Chem. Soc. 121 (1999) 4196.
[18] K.S. Suslick, S.-B. Choe, A.A. Cichowlas, M.W. Grinstaff, Nature 353 (1991) 414.
[19] R.A. Salkar, P. Jeevanandam, S.T. Aruna, Yuri Koltypin, A. Gedanken, J. Mater. Chem. 9 (1999) 1333.
[20] J. Zhu, Z. Lu, T.S. Aruna, D. Aurbach, A. Gedanken, Chem. Mater. 12 (2000) 2557.
[21] S. Ramesh, Yu. Koltypin, R. Prozorov, A. Gedanken, Chem. Mater. 9 (1997) 546.
[22] V.G. Pol, R. Reisfeld, A. Gedanken, Chem. Mater. 14 (2002) 3920.
[23] V.G. Pol, M. Motiei, A. Gedanken, J. Calderon-Moreno, Y. Mastai, Chem. Mater. 15 (2003) 1378.
[24] K.S. Suslick, G.J. Price, Annu. Rev. Mater. Sci. 29 (1999) 295.
[25] I. Mastai, G. Hodes, R. Polsky, Yu. Koltypin, A. Gedanken, J. Am. Chem. Soc. 121 (1999) 10047.
[26] T. Aoshima, K. Okahara, C. Kiyohara, K. Shizuka, J. Power Sources 97–98 (2001) 377.
[27] D. Aurbach, J. Power Sources 89 (2000) 206.